



ELSEVIER

Available online at www.sciencedirect.com

SCIENCE @ DIRECT®

Nuclear Instruments and Methods in Physics Research B 199 (2003) 469–474

NIM B
Beam Interactions
with Materials & Atoms

www.elsevier.com/locate/nimb

Electromigration in integrated circuit interconnects studied by X-ray microscopy

G. Schneider ^{a,*}, G. Denbeaux ^a, E. Anderson ^a, W. Bates ^a,
F. Salmassi ^a, P. Nachimuthu ^a, A. Pearson ^a, D. Richardson ^a,
D. Hambach ^b, N. Hoffmann ^c, W. Hasse ^c, K. Hoffmann ^d

^a Center for X-ray Optics, Lawrence Berkeley National Laboratory, 1 Cyclotron Road Mail Stop 2-400, Berkeley, CA 94720, USA

^b Institut für Röntgenphysik, Universität Göttingen, Geiststraße 11, D-37073 Göttingen, Germany

^c Institut für Halbleitertechnologie und Werkstoffe der Elektrotechnik, Universität Hannover, Appelstraße 11, D-37073 Göttingen, Germany

^d Micronas GmbH, Hans-Bunte-Str. 19, D-79108 Freiburg, Germany

Abstract

To study mass transport phenomena in advanced microelectronic devices with X-rays requires penetration of dielectric and Si layers up to 30 μm thick. X-ray imaging at 1.8 keV photon energy provides a high amplitude contrast between Cu or Al interconnects and dielectric layers and can penetrate through the required thickness. To perform X-ray microscopy at 1.8 keV, a new Ru/Si multilayer was designed for the transmission X-ray microscope XM-1 installed at the Advanced Light Source in Berkeley. The mass flow in a passivated Cu interconnect was studied at current densities up to 10^7 A/cm². In addition, we demonstrated the high material contrast from different elements in integrated circuits with a resolution of about 40 nm.

© 2002 Elsevier Science B.V. All rights reserved.

PACS: 66.30.Qa; 85.40.Ls; 07.85.Tt; 42.30.Wb

Keywords: X-ray imaging; Zone plates; Interconnects; Electromigration

1. Introduction

The challenge in designing integrated circuits (ICs) is to ensure reliability while squeezing as much performance out of the process as possible. As the semiconductor industry produces microprocessors which operate at frequencies up to

several GHz, about 100 million transistors have to be integrated. The interconnect structures in advanced microelectronic devices are currently 200 nm wide and operate at high current densities of nearly 10^6 A/cm² without excessive Joule heating, because the heat is dissipated into the bulk Si and the dielectric layers surrounding the thin film conductors. At these current densities, which are at least two orders of magnitude higher than in traditional bulk wires, one of the major failure mechanisms is electromigration (EM), i.e. the transport of atoms in an interconnect along the

* Corresponding author. Tel.: +1-510-486-7052; fax: +1-510-486-4955.

E-mail address: gschneil@gwdg.de (G. Schneider).

direction of electron flow. The material transport can result in voids in the wire leading to open circuit failures, as well as hillocks which extrude from the original interconnect causing short circuits.

In place of Al, Cu is increasingly being employed as an interconnect material due to its higher conductivity and better resistance against EM failure. Cu interconnects have to be encapsulated with special metallic or dielectric barriers to prevent Cu diffusion into the silicon as Cu does not form an adherent oxide diffusion barrier like Al. Therefore, the interfaces between Cu and the surrounding barriers could be an easy EM pathway and interface or surface diffusion may be very important for the EM behavior of a Cu multilevel metallization system [1,2]. Failures in interconnects involve a complicated process of nucleation, growth, motion and shape change of voids, which depends heavily on the microstructure and composition of the metal. Current research has shifted towards gaining an improved understanding of the physics behind the void nucleation and growth processes [3].

In a passivated interconnect, the mass flow due to EM is constrained by encapsulation. This leads to a high mechanical stress in the interconnect that influences the material transport significantly. Furthermore, for accelerated failure measurements, the temperature distribution in the device under test depends strongly on the layers surrounding the stressed interconnect. Thus, realistic in situ observation of EM should be done in an intact layer system including all barriers and passivation layers.

Due to continued reduction of feature sizes, the importance of interconnects in chip design is growing, and EM has become one of the principal limiting factors in achieving higher performance microprocessors. An understanding of the parameters affecting EM is very important when designing advanced ICs. Thus EM in interconnects must be studied in a realistic IC environment. For this purpose an imaging technique is required which maintains high spatial resolution while penetrating through several microns of dielectrics. Optical microscopy does not provide the necessary spatial resolution and transmission electron micro-

scopy has the disadvantage that only very thin layers can be studied. Surface-sensitive techniques like scanning electron microscopy or atomic force microscopy require destructive sample preparation which prevents real-time, in situ studies of material transport processes within an intact layer system. These techniques do not permit EM studies under the conditions relevant to operating ICs.

The limitations of the conventional imaging techniques can be overcome when using X-rays for EM studies [4]. Currently, X-ray microscopes operating in the soft X-ray region provide a spatial resolution of about an order of magnitude better than visible light microscopes. In addition, as shown in Fig. 1, X-rays can penetrate many micrometer thick substrates and due to their unique interactions with matter, they provide a natural image contrast between different elements, e.g. Cu in SiO_2 . Also it was shown that the number of photons required to detect a void or hillock in an interconnect is at a minimum at a photon energy $E_{\text{ph}} = 1.8 \text{ keV}$ [4]. The photon flux emitted by a bending magnet installed in an electron storage ring like the ALS operating at 1.9 GeV electron

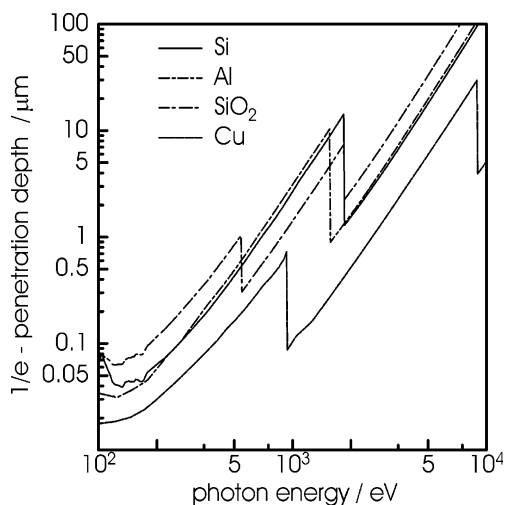


Fig. 1. Thickness of Si, Al, SiO_2 and Cu layers for $1/e$ -transmission as a function of photon energy. Relevant layer thicknesses for interconnect studies are in the micrometer range. As can be seen from the plot, Si at the low-energy side of its K-absorption edge at 1.839 keV is much more transparent than Cu. At this photon energy, passivated Cu interconnects provide a high absorption contrast in X-ray microscope images.

energy is close to its maximum at this photon energy. However, depending on the sample thickness, much higher photon energies can advantageously be used for imaging IC structures [5].

2. Experimental setup

The full-field transmission X-ray microscope XM-1 operating at the ALS in Berkeley was designed for imaging samples with soft X-rays below $E_{\text{ph}} = 0.8$ keV photon energy [6,7]. Its X-ray optical setup is shown in Fig. 2. Previously, a Ni mirror operating at fixed angular position of 3° was used to block photons with energies higher than $E_{\text{ph}} = 0.8$ keV. In order to use the microscope for interconnect studies at $E_{\text{ph}} = 1.8$ keV, we designed a Ru/Si multilayer with $N = 45$ periods, a period of 15 nm and a ratio (high-Z-material layer thickness/period) $\gamma = 0.4$. Fig. 3 shows the reflectivity for the new Ru/Si multilayer and the previously used Ni mirror versus photon energy. As can

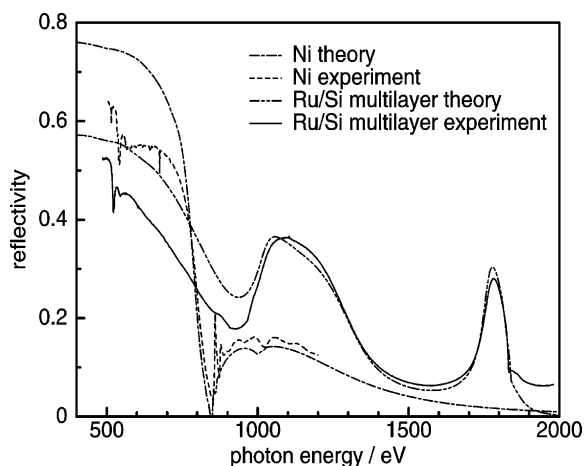


Fig. 3. Reflectivity of the Ru/Si multilayer and the previously used Ni mirror in the photon energy range up to 2 keV at a fixed grazing incidence angle of 3° . The experimental data of the Ru/Si multilayer reflectivity are in good agreement with the theoretical calculations. It also shows that the multilayer provides sufficient reflectivity over the whole energy range, whereas the previously used Ni mirror is only suited for imaging below 0.8 keV photon energy.

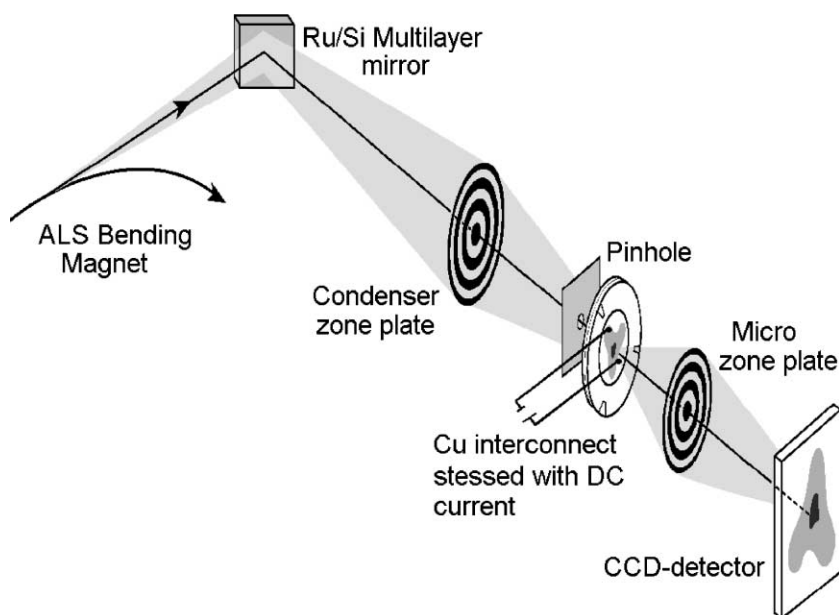


Fig. 2. Schematic of the full-field transmission X-ray microscope XM-1 used for the EM studies of buried Cu interconnects. The bending magnet radiation is reflected at a 3° incidence by a Ru/Si multilayer and then monochromatized by a condenser zone plate which illuminates the sample at $E_{\text{ph}} = 1.8$ keV photon energy with an energy bandwidth $E/\Delta E \approx 400$. The diffracted X-rays are collected by an objective zone plate which forms an enlarged image of the sample on a directly illuminated back-thinned CCD-camera.

be seen from the plot, the reflectivity of the Ru/Si multilayer at E_{ph} about 0.5 keV is only slightly lower than the reflectivity of the Ni mirror. Note the reflectivity peak of the multilayer at $E_{\text{ph}} = 1.8$ keV photon energy. With the new multilayer it is now possible to perform microscopy experiments at photon energies up to the K-absorption edge of Si without changing the incidence angle of the mirror.

The bending magnet radiation is reflected by the mirror and monochromatized by a condenser zone plate, which also illuminates the sample. Because the focal length of zone plates increases linearly with photon energy, a new condenser zone plate (CZP) was manufactured with a diameter of 8 mm and an outermost zone width of 55 nm. This CZP is fully illuminated with the bending magnet radiation at $E_{\text{ph}} = 1.8$ keV. To match the geometrical requirements of the existing TXM for imaging at this photon energy and to achieve a sufficiently large magnification, we also designed new objective zone plates with a lower number of zones and a shorter focal length. The maximum distance from the sample to the detector plane is 2 m and the pixel size of the CCD detector is 24 μm . Therefore, we used objective zone plates with only

230 zones, 35 nm outermost zone width and a focal length of 1.6 mm at $E_{\text{ph}} = 1.8$ keV to nearly fulfill the sampling theorem. Under these conditions the pixel size in the X-ray images is 19 nm, which fits with the obtainable resolution of about 40 nm determined by the objective zone plate. Using a bilayer process and e-beam lithography, both condenser and objective zone plate were manufactured in Ni having a zone thickness of about 180 nm [8,9].

3. X-ray imaging of microprocessor structures

To demonstrate that different microstructures can be distinguished in X-ray microscope images of an intact processor, we studied an intact IC with three levels of interconnects which are made from a Si/WSi sandwich and from an AlCu alloy. The only necessary preparation step was thinning of the silicon wafer from the backside to about 10 μm thickness. Note that this leaves the device in working order for eventual further electrical testing. Fig. 4 shows X-ray micrographs of arbitrary parts of the IC. Several chip structures at different metallization levels can be identified (arrows indi-

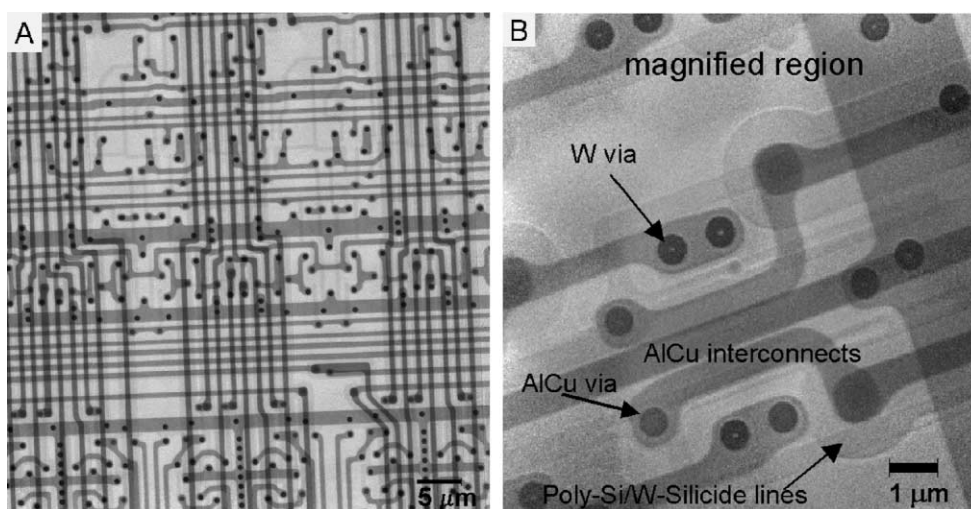


Fig. 4. (A) X-ray micrograph showing an overview of an intact IC with three metallic layers. The dark gray lines indicate structures of an AlCu metallization layer. The light gray lines show Si/WSi lines, which have lower contrast than AlCu interconnects at $E_{\text{ph}} = 1.8$ keV. (B) Magnified region of the IC showing details of the metallization layers, e.g. the central holes in the W vias with less than 80 nm in diameter.

cate some examples). The Si/WSi lines have a thickness of about 0.5 μm . Furthermore, two layers of the AlCu metallization are visible (see Fig. 4(A)), each of about 0.5 μm thickness. They are separated from each other and from the Si/WSi lines by dielectric films with 1 μm thickness.

The minimum line width of the interconnects is 0.45 μm in this chip. Also two different types of vias can be distinguished by their different X-ray absorption characteristics. Tungsten vias connect the Si/WSi lines with the first AlCu metallization layer (see Fig. 4(B)). The diameter of the W plugs is 0.5 μm . Some of the W plugs in Fig. 4(B) show a bright central spot. It is caused by the specific growth mechanism of the W plugs from the edge to the center of the contact holes during the plug formation by CVD. Some of them end up with a small cavity in the center, which are resolved in the X-ray micrograph in Fig. 4(B). The two AlCu metallization layers are interconnected by AlCu vias, which are less absorbing for $E_{\text{ph}} = 1.8$ keV X-rays and therefore appear brighter in the X-ray micrograph shown in Fig. 4. This example demonstrates the high material contrast of metallization layers and IC structures in X-ray microscope images as well as the fact that high resolution images with about 40 nm resolution can be obtained at photon energies above $E_{\text{ph}} = 1$ keV. For future applications this can be combined with computed tomography to provide three-dimensional element information and to locate hidden particles. Thus, X-ray microscopy is also a powerful new technique for defect analysis.

4. Electromigration in Cu interconnects

For the EM experiment, Cu lines using the well-known NIST test structure (ASTM standard F 1259M-96) were investigated [10]. A schematic cross-section of the test structure is shown in Fig. 5. The total thickness of the passivation layers is about 1.5 μm and the silicon wafer was thinned to a thickness of about 5 μm . To visualize the dynamics of EM, the Cu line was stressed by applying a DC current of 49.8 mA. During 30 min of observation, a time sequence of images – each with an exposure time of about 1 s – was recorded with

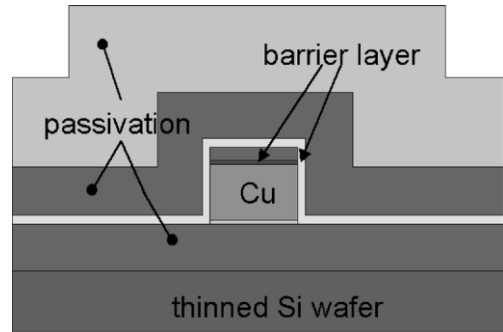


Fig. 5. Cross-section of the passivated Cu interconnect layer system used for the EM experiment [4]. The thickness of the Cu layer is 350 nm and its linewidth is 600 nm. The silicon wafer was thinned by wet etching with KOH solution.

the TXM, directly displaying the formation of voids. Selected X-ray micrographs of the transition region between the wide and the small part of the test structure at the cathode site are shown in Fig. 6. For the stress conditions used, the mass flow divergences are mainly caused by temperature gradients, and in this regime forming of voids has to be expected. Very fast and significant changes of the failure site in the last 2 min (see Fig. 6, two right images) of the experiment show the effects of the rapidly increasing current density which is due to a decreasing cross-section of the interconnect (see Fig. 6). In the X-ray micrographs presented here, the accuracy of mass displacement

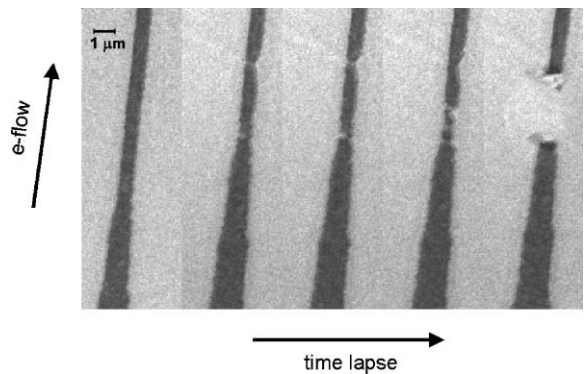


Fig. 6. X-ray micrographs taken with XM-1 at a photon energy of 1.8 keV visualizing the mass transport by EM in a passivated Cu interconnect. The current densities were increased up to 10^7 A/cm² during 30 min of image recording.

measurement is about 60 nm. Because of the limited dynamical range of the CCD-camera at 1.8 keV, up to now the obtainable resolution is mainly shot-noise limited and therefore, does not reach the resolution limit provided by the X-ray objective. To overcome this limitation, we plan to convert the X-rays with a phosphor screen into visible light, which is then imaged with a visible light objective onto the CCD-camera. This will provide an increased dynamic range and will avoid the radiation damage problem that occurs during direct illumination of the CCD with 1.8 keV X-rays.

In summary, XM-1 is the first full-field high resolution X-ray microscope operating at a bending magnet source at photon energies in the keV range. We have demonstrated that a full-field transmission X-ray microscope operating at 1.8 keV photon energies allows detection of passivated interconnects made from Cu or AlCu as well as vias. It was also shown that the mass flow caused by electromigration can be studied in situ.

In the future, X-ray imaging and microdiffraction could be combined to provide simultaneous time-resolved data about the mass flow as well as the corresponding grain orientation. Furthermore, we conclude that X-ray imaging is suited to detect and analyze failures in integrated circuits without special preparation steps, especially when combined with nano-tomography to obtain three-dimensional reconstructions of microprocessor structures. By improving the detector and the nanostructuring process for the zone plate objectives, it seems to be realistic to achieve a spatial resolution of better than 30 nm.

Acknowledgements

We greatly acknowledge D. Attwood for supporting this work as well as D. Olynick and B. Harteneck for manufacturing the zone plates. This work is funded in part by the US Department of energy, office of Basic Energy Science under contract no. DE-AC03-76SF00098 and the Deutsche Forschungsgemeinschaft (DFG) under contract no. SCHN 529/1-1.

References

- [1] L. Arnaud, G. Tartavel, T. Berger, D. Mariolle, Y. Gobil, I. Touet, in: Proceedings 37th International Reliability Physics Symposium 1999, San Diego, 1999.
- [2] C.-K. Hu, R. Rosenberg, K.Y. Lee, *Appl. Phys. Lett.* 74 (1999) 2945.
- [3] J.R. Lloyd, *J. Phys. D: Appl. Phys.* 32 (1999) R109.
- [4] G. Schneider, D. Hambach, B. Kaulich, N. Hoffmann, W. Hasse, B. Niemann, J. Susini, *Appl. Phys. Lett.* 78 (2001) 1936.
- [5] W. Yun et al., in: W. Meyer-Ilse, D. Attwood (Eds.), Proceedings of the Sixth International Conference, American Institute of Physics, 2000.
- [6] W. Meyer-Ilse, H. Meddecki, L. Jochum, D. Attwood, C. Magowan, R. Balhorn, M. Moronne, D. Rudolph, G. Schmahl, *Synchrotron Radiat. News* 8 (1995) 23.
- [7] G. Denbeaux, E. Anderson, W. Chao, T. Eimüller, L. Johnson, M. Köhler, C. Larabell, M. LeGros, P. Fischer, A. Pearson, G. Schütz, D. Yager, D. Attwood, *Nucl. Instr. Meth. A* 467–468 (2001) 841.
- [8] D. Olynick, E. Anderson, B. Harteneck, E. Veklerov, *J. Vac. Sci. Technol. B* 19 (6) (2001) 2896.
- [9] E.H. Anderson et al., *J. Vac. Sci. Technol. B* 18 (6) (2000) 2970.
- [10] ASTM standard F 1259M-96, Annual book of ASTM standards, American Society for Testing and Materials, 1996.